# Atypical PWM for Maximizing 2L-VSI DC-Bus Utilization in Inverter-Based Microgrids with Ancillary Services

Aswad Adib[1], Jacob Lamb[2], and Behrooz Mirafzal[1]
[1]Department of Electrical and Computer Engineering, Kansas State University, Manhattan, KS, USA
[2]Rockwell Automation, Mequon, WI, USA
aswadadib@ksu.edu; jmlamb@ra.rockwell.com; mirafzal@ksu.edu

*Abstract*— **Three-phase microgrid-interactive inverters are expected to provide a range of ancillary services, with negative-sequence current compensation being particularly prominent. However, unbalanced pulse width modulation (PWM) references may be generated when providing these services. Since references used by carrier-based PWM techniques cannot exceed the dc-bus voltage defined limits without causing over-modulation, the maximum positive-sequence voltage microgrid-interactive inverters can generate may therefore be diminished. This will in turn reduce the maximum active- and reactive-power that the inverter could otherwise provide, unless PWM references are adjusted. In this paper, an atypical PWM method is proposed for maximizing dc-bus utilization of microgrid-interactive two-level voltage source inverters (2L-VSI) operating under unbalanced conditions. Through the injection of a common-mode component computed based on instantaneous reference magnitudes, the proposed method increases the maximum active- and reactive-power that a 2L-VSI can deliver when providing negative-sequence current compensation. The validity of the proposed technique is verified through simulation, as well as experimental data obtained using a 208V three phase grid-connected 2L-VSI.**

***Keywords—Atypical PWM, DC-bus utilization, microgrids, negative-sequence compensation, ancillary (auxiliary) services.***

## I. INTRODUCTION

Traditional power systems are characterized by unidirectional flow of power from large power plants to load centers over a great distance. Recently with the increased penetration of renewable energy resources the load centers now have localized power generation in the form of distributed generation (DG) units such as rooftop photovoltaic (PV), small wind turbines, fuel cells, micro-turbines and battery energy storage systems to name a few. This arrangement is called a microgrid, where a group of DG units can either work in conjunction with the utility in grid-connected mode or isolated from the utility in stand-alone mode to provide power to its associated loads [1], [2]. The enabling technology of these DG units is an inverter-based power electronic interface, with the two-level voltage source inverter (2L-VSI) being the most prevalent option. Depending on whether the microgrid is grid-connected or islanded, the 2L-VSI can operate in PQ mode to regulate the flow of active and reactive power to the load or in voltage control mode to regulate the voltage and frequency at the load terminal, respectively. In addition to providing power, inclusion of 2L-VSIs enables the microgrid to provide a range of ancillary (or auxiliary) services, some of which are, but not limited to, voltage support, power factor correction, harmonic compensation and unbalance compensation [3]-[5]. Due to their small scale, microgrids are subject to a significant degree of unbalanced [6], making negative-sequence current compensation a particularly important ancillary service for microgrids.

Traditionally negative-sequence compensation has been provided through external power conditioning devices such as STATCOMs and active filters [7]-[10]. However, as both these technologies are inverter based, inverters are capable of providing these services following the same operating principle. Several techniques have been proposed in literature to compensate negative-sequence components in grid currents using inverters, primarily through the implementation of new control strategies [11]-[14]. In [11], the authors investigate two different control strategies for negative-sequence compensation with particular emphasis on minimizing active power oscillation. Unbalance compensation under polluted grid conditions has also been studied using a gain scheduling multi-resonant controller [12], a non-linear controller based on back stepping control and high-order sliding mode differentiator [13], and a control strategy employing third-order sinusoidal signal integrator-based frequency adaptive filter [14]. However, some limitations such ancillary services impose on the 2L-VSI operating range is yet to be investigated. Providing negative-sequence current compensation may require unbalanced 2L-VSI line-to-neutral voltages, as measured from a line output to the inverter's dc-bus midpoint [15]. Since line-to-neutral voltages cannot exceed dc-bus voltage limits without causing over-modulation, the inverter's maximum positive-sequence voltage component must therefore be reduced. Accordingly, if line-to-neutral voltages are not adjusted, the maximum active- and reactive power that a 2L-VSI can supply may be diminished when the inverter provides ancillary services.

To increase the maximum active- and reactive-power a grid-interactive 2L-VSI can deliver when providing negative-

This work was supported in part by the National Science Foundation under Grant No. ECCS-1351665.

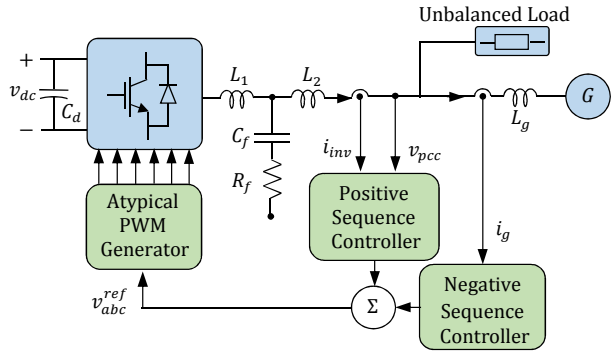


Fig. 1. Schematic diagram of a grid-connected 2L-VSI supplying an unbalanced load.

sequence compensation, an atypical pulse width modulation (PWM) method for enabling maximum dc-bus utilization by injecting a common-mode component into PWM references is presented in this paper. When utilizing carrier-based PWM techniques, preferred due to implementation simplicity and a well-defined harmonic spectrum [16], the injection of a common-mode component is facilitated as PWM references define line-to-neutral voltages. For 2L-VSIs, a common-mode component in the line-to-neutral voltages may be designed to improve inverter performance, e.g. decreasing switching losses or increasing the linear modulation range [16], [17]. Common-mode injection techniques typically focus on balanced inverter conditions [16], [18], with little attention paid to inverters operating under the unbalanced conditions typical for microgrid operation, a shortcoming addressed by this paper.

In addition to this introduction, this paper contains five sections. In Section II, the need for ancillary services and the grid-connected 2L-VSI system is reviewed. In Section III, the carrier-based atypical PWM scheme is introduced. The developed PWM technique is verified through simulation and experimental data presented in Sections IV and V, respectively. Concluding remarks are provided in Section VI, along with an outline of future works.

## II. Ancillary Services and System Description

As single-phase DG units penetration increases in the grid, three-phase systems that are typically balanced have the potential to become unbalanced as the load demand of each phase fluctuates. This issue is exacerbated by the topology of power distribution systems in the US, where single electrical phases supply geographically distinct areas, as well as, in islanded microgrids. If the resulting asymmetric load variations are severe enough, they can potentially saturate three-phase transformers, cause malfunctions in protection devices, and damage diesel synchronous generators [19], [20]. To alleviate this three-phase power imbalance, a three-phase smart 2L-VSI controlled energy storage system can be utilized to balance the current drawn from the grid or from synchronous generators in islanded microgrids. Through negative-sequence compensation, the 2L-VSIs can provide the negative-sequence current requirements of their associated loads. However, this restricts the positive-sequence voltage a 2L-VSI can generate which in turn limits the active- and reactive-power a 2L-VSI can provide.

The schematic diagram of a grid-connected 2L-VSI is shown in Fig. 1. As illustrated in Fig. 1, grid-connected 2L-VSI are typically coupled to the grid via an LCL filter, with inverter-side inductance $L_1$, grid-side inductance $L_2$, and Δ-connected capacitors, $C_f$ with series damping resistors $R_f$. The positive-sequence current component of the 2L-VSI is regulated by two cascaded PQ-controllers in the synchronously rotating $dq$ frame of reference [21], [22]. This approach allows independent control of active- (P) and reactive-power (Q) being supplied.

The positive-sequence controller requires measurement of two line-to-line voltages ($v_{pcc}$) from the point of common coupling (PCC) and two line currents ($i_{inv}$) after the filter capacitors as feedback signals as shown in Fig. 1. The line-to-line voltages are also used as grid voltage feedforward for better dynamic performance of the controller. The q- and d-components of the measured signals are calculated with $v_{pcc}$ as reference. A phase locked loop (PLL) is used to measure the instantaneous phase angle of the PCC voltage.

To provide negative-sequence compensation, a separate set of independent controllers are utilized. These negative-sequence controllers require the negative-sequence component of currents delivered by the grid to be computed. Based on the grid's negative-sequence component, caused by the unbalanced load shown in Fig. 1, a compensating current is injected by the inverter. The output of both set of controllers are added to create PWM references. The resulting references may be asymmetrical, making traditional common-mode injection techniques, such as third-harmonic injection, unsuitable. A more flexible common-mode injection approach, which utilizes instantaneous reference values, is proposed in the next section.

## III. PWM Reference Common-Mode Injection

In this section, the atypical PWM scheme for maximizing dc-bus utilization of a 2L-VSI is derived. For a typical carrier-based PWM, the modulation signal can be expressed as

$$v_x = \frac{m v_{dc}}{2} \sin(\omega t - \varphi_x), \qquad x \in \{a, b, c\} \tag{1}$$

where, $v_{dc}$ is the dc-bus voltage, $m$ is the modulation index, and $\varphi_x$ is 0, $2\pi/3$ and $4\pi/3$ for phases a, b and c, respectively. A 2L-VSI is in the linear modulation range if $|\hat{v}_x| \leq v_{dc}/2$, where $\hat{v}_x$ is the peak phase-x PWM reference. Therefore, when operating in the linear modulation range, the 2L-VSI's maximum line-to-line voltages are obtained when $|\hat{v}_x| = v_{dc}/2$ for some $x \in \{a, b, c\}$ if no common-mode component is used to adjust PWM references. Accordingly, the PWM reference's maximum positive sequence component is reduced when a negative-sequence component is required. To mitigate this effect, references can be used to define a common-mode component, allowing adjusted references to be generated.

For a set of references at angle $\theta_0$, a common-mode component is required when $|v_x(\theta_0)| > v_{dc}/2$ for some $x \in$

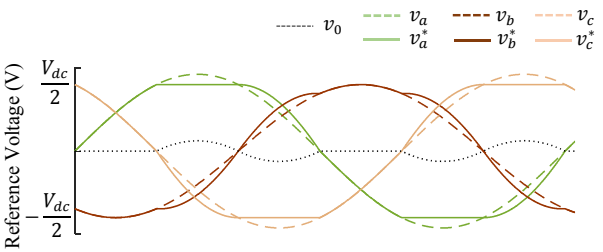


Fig. 2. Atypical PWM references, $v_x^*$, generated using the proposed technique, compared to the unadjusted references, $v_x$.

$\{a, b, c\}$. Defining $k$ as the phase for which over-modulation occurs

$$k = \underset{x \in \{a,b,c\}}{argmax}\ (|v_x(\theta_0)|), \tag{2}$$

the minimum common-mode component placing $v_k(\theta_0)$ in the linear modulation range is computed as,

$$v_o(\theta_0) = \begin{cases} v_k(\theta_0) + v_{dc}/2 & v_k(\theta_0) < -v_{dc}/2 \\ v_k(\theta_0) - v_{dc}/2 & v_k(\theta_0) > v_{dc}/2 \\ 0 & \text{otherwise.} \end{cases} \tag{3}$$

The common-mode component computed via (3), is then used to generate modified PWM references as,

$$v_x^*(\theta_0) = v_x(\theta_0) - v_o(\theta_0), \qquad x \in \{a, b, c\}. \tag{4}$$

Atypical PWM references generated using (4) is plotted in Fig. 2 and compared with the unadjusted PWM references which contain positive and negative-sequence components. The atypical references may appear distorted and clamped as shown in Fig. 2. However, by injecting the same common-mode component for all the phases ensures that the distortion does not appear in the line-to-line voltages. It can also be seen from Fig. 2 that the regular PWM signals are in the over-modulation region while the PWM generated using (4) remains clamped at $v_{dc}/2$. Since, for $|v_k(\theta_0) > | v_{dc}/2$, applying $v_o(\theta_0)$ as in (3) and (4) guarantees $|v_k(\theta_0) - v_o(\theta_0)| = |v_k^*(\theta_0)| = v_{dc}/2$.

The $v_x^*(\theta_0)$ are guaranteed to be within the linear-modulation range provided $|v_x(\theta_0) - v_y(\theta_0)| \leq v_{dc}$ for all $x, y \in \{a, b, c\}$. Compared to the case where PWM references contain no common-mode component, the increase in dc-bus utilization when utilizing the proposed technique is dependent upon the references' negative-sequence content. The proposed scheme does not influence the voltage reference generation through the controller nor does it directly generate the gate pulses. It operates as an intermediary between reference voltage and gate pulse creation. As a result, the proposed atypical scheme can work in conjunction with any control system and carrier-based PWMs.

TABLE I
SIMULATION PARAMETERS

| | |
|---|---|
| PWM Carrier Frequency | 10 kHz |
| Fundamental Frequency | 60 Hz |
| $V_{LL,rms}$ | 208 V |
| $v_{dc}$ | 350 V |
| $L_1$ | 1.0 mH |
| $C_f(\Delta)$ | 10.0 µF |
| $R_f$ | 3.3 Ω |
| $L_2$ | 1.0 mH |
| $C_d$ | 1800 µF |

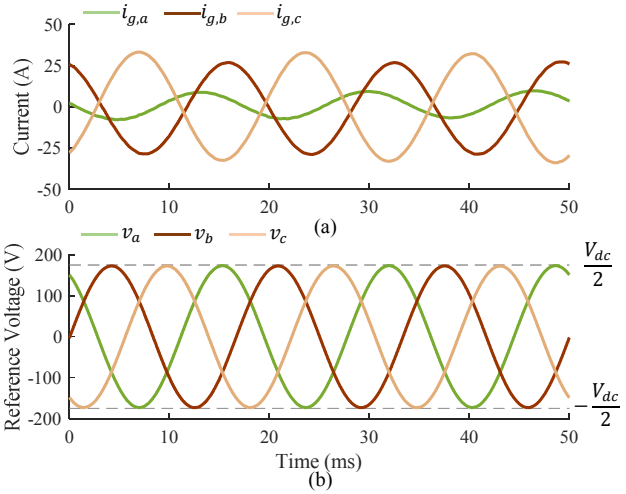


Fig. 3. (a) Three-phase grid currents and (b) PWM references when the 2L-VSI is supplying 18 kW power to an unbalanced load with no negative-sequence compensation.

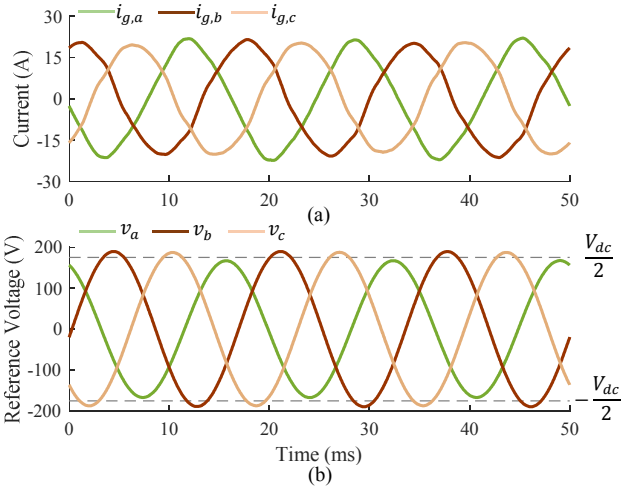


Fig. 4. (a) Three-phase grid currents and (b) PWM references when the 2L-VSI is supplying 18 kW power to an unbalanced load while providing negative-sequence compensation.

## IV. SIMULATION RESULTS

In this section, the performance of the atypical PWM scheme developed in the previous section is evaluated through MATLAB/Simulink simulation studies. The parameters used for simulation can be found in Table I. Furthermore, for the unbalanced load a Δ-connected 20kW resistive load with $R_{ab} = 5.408\Omega, R_{bc} = 5.408\Omega$ and $R_{ca} = 10.816\Omega$ was used. A 208 $V_{rms}$ three-phase voltage source with an impedance of $0.107\Omega$ and a X/R ratio of 0.4 was used for grid connection.

In the first scenario, the grid-tied 2L-VSI is supplying 18 kW power to the unbalanced load, with no negative-sequence

compensation provided. The resulting grid currents and the PWM references are shown in Fig. 3. Due to the unbalanced load, the grid current has a significant negative-sequence component. On the other hand, the PWM references are balanced, as only positive-sequence controller of 2L-VSI is operational.

Attempting to maintain the delivery of 18 kW at unity power factor and activating negative-sequence compensation results in unbalanced PWM waveforms, as shown in Fig. 4. Because these unbalanced waveforms have peak values above $v_{dc}/2$, the inverter operates in the overmodulation region. Low order harmonic content, which is typical in the over-modulation region, causes noticeably distorted grid currents.

To enable negative-sequence compensation while operating the inverter in the linear modulation region, the inverter's positive-sequence component must be reduced, which requires the power delivered by the inverter to be reduced to 12 kW,

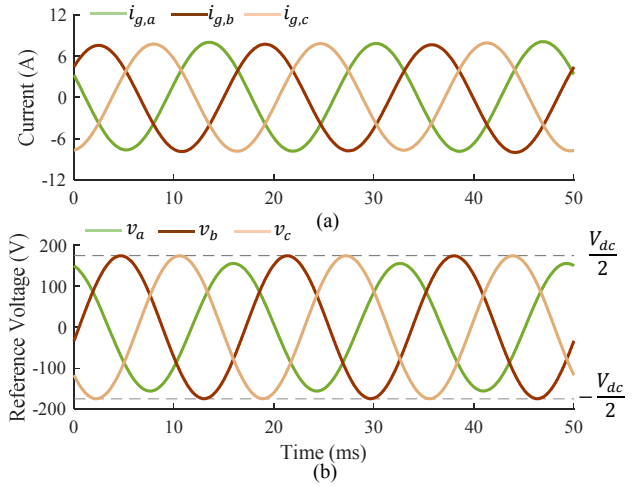


Fig. 5. (a) Three-phase grid currents and (b) PWM references when the 2L-VSI is supplying 12 kW power to an unbalanced load with negative-sequence compensation.

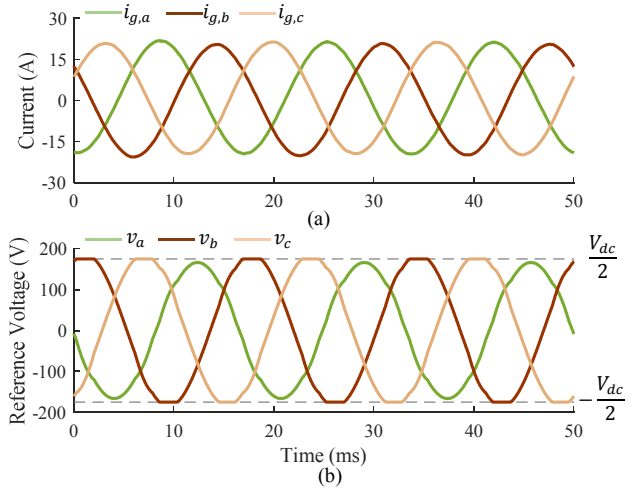


Fig. 6. (a) Three-phase grid currents and (b) PWM references when the 2L-VSI is supplying 18 kW power to an unbalanced load with negative-sequence compensation while employing atypical PWM scheme.

TABLE II
GRID CURRENT THD (%) FOR VARYING DEGREE OF LOAD UNBALANCE

| $R_{ca}$ \ $R_{bc}$ | 70(%) | 85(%) | 100(%) | 115(%) | 130(%) |
|---|---|---|---|---|---|
| 70(%) | 1.13 | 1.30 | 1.24 | 1.25 | 1.28 |
| 85(%) | 1.48 | 1.34 | 1.62 | 1.41 | 1.33 |
| 100(%) | 1.38 | 1.43 | 1.34 | 1.38 | 1.33 |
| 115(%) | 1.45 | 1.43 | 1.26 | 1.31 | 1.22 |
| 130(%) | 1.62 | 1.76 | 1.34 | 1.38 | 1.22 |

delivered at unity power factor. The resulting grid currents and PWM references are shown in Fig. 5. The proposed atypical PWM scheme can be utilized as an alternative technique to enable linear-region modulation without requiring this significant decrease in the delivered active power.

Grid currents and PWM waveforms shown in Fig. 6 were obtained with the inverter delivering 18 kW at unity power factor, with negative-sequence compensation and the proposed atypical PWM scheme activated. The resulting grid currents are balanced, as expected from the negative-sequence compensation. Further, the grid currents contain no low order harmonic content, as the atypical PWM technique keeps all references in the linear modulation region.

Next, the performance of the atypical PWM scheme was tested under a range of load unbalance. Delta-connected resistances $R_{bc}$ and $R_{ca}$ were independently varied up to 30% from a nominal resistance of 6.5 Ω, selected to create a 20 kW load under nominal condition. For all tests, the 2L-VSI delivered 20 kW at unity power factor and provided negative-sequence compensation. For each unbalance configuration, the total harmonic distortion (THD) of three phases of the grid currents were calculated and then averaged, and results are provided in Table II. The calculated THD are within acceptable limits for all load unbalance cases considered, demonstrating the efficacy of the proposed PWM scheme.

## V. EXPERIMENTAL VERIFICATION

In this section, the proposed atypical PWM scheme is verified via data collected using a grid-connected 2L-VSI system supplying a 2 kW unbalanced load with $R_a = 24\Omega, R_b = 24\Omega$, and $R_c = 31\Omega$. The 2L-VSI used for experimental data collection was an Allen-Bradley Powerflex

TABLE III
EXPERIMENTAL PARAMETERS

| | |
|---|---|
| PWM Carrier Frequency | 6.25 kHz |
| Fundamental Frequency | 60 Hz |
| $V_{LL,rms}$ | 208 V |
| $L_1$ | 1.0 mH |
| $C_f(\Delta)$ | 5.0 µF |
| $R_f$ | 3.3 Ω |
| $L_2$ | 0.5 mH |
| $C_d$ | 1800 µF |

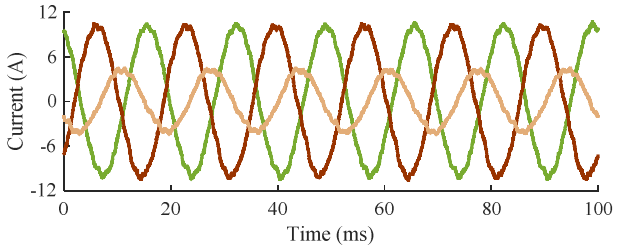


Fig. 8. Experimentally obtained grid currents when $V_{dc} = 375V$ and no negative-sequence compensation is used.

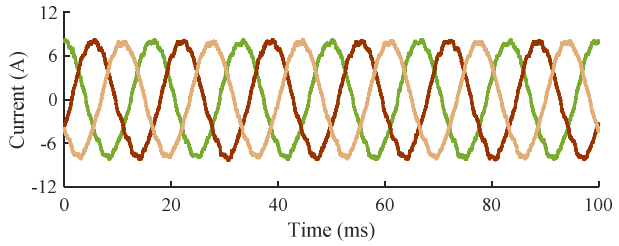


Fig. 9. Experimentally obtained grid currents when $V_{dc} = 375V$ and negative-sequence compensation is provided by the 2L-VSI.

755, controlled by PWM references generated using a dSpace CP1103 control board. Gate signals were generated using Altera Cyclone III FPGA coupled to the dSpace board [23], [24]. For all data collected, the inverter was set to deliver 500W due to constraints of the laboratory equipment. The experimental setup is shown in Fig. 7. The experimental data was collected using a LeCroy Waverunner 64Xi-A oscilloscope with ADP300 differential voltage probes and CP030 current probes for voltage and current measurement, respectively. The data was collected at a sampling frequency of 100kHz and plotted using MATLAB.

Using a 375 V dc-bus voltage, the grid currents shown in Fig. 8 were obtained when the inverter provided the desired 500 W but did not provide negative-sequence compensation. Since this unbalanced current can cause deleterious effects in microgrid scale generators, implementing negative-sequence

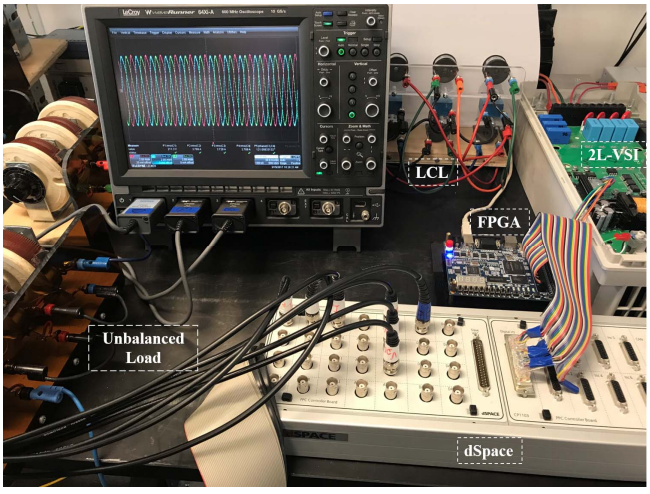


Fig 7. Hardware setup used for the experimental scenarios in Section IV.

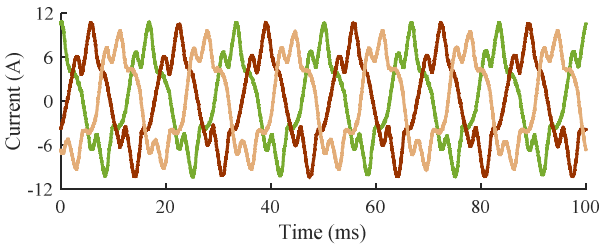


Fig. 10. Experimentally obtained grid currents when $V_{dc} = 320V$ and negative-sequence compensation is used without utilizing proposed atypical PWM scheme.

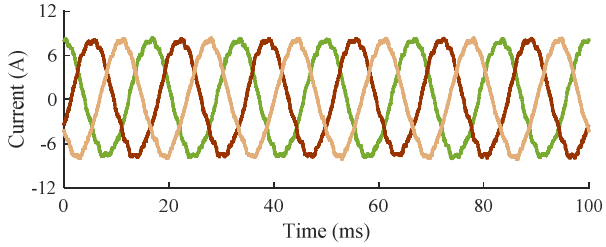


Fig. 11. Experimentally obtained grid currents when $V_{dc} = 320V$, obtained when negative-sequence compensation is used utilizing the proposed atypical PWM scheme.

compensation may be beneficial. The grid currents shown in Fig. 9 were obtained when the inverter was made to provide 500 W as well as negative-sequence compensation. For data shown in Figs. 8 and 9, the proposed atypical PWM scheme was not utilized.

To demonstrate the efficacy of the proposed technique when negative-sequence compensation is provided, grid currents were measured for a 320 V dc-bus voltage. The results obtained with and without using the proposed scheme are shown in Figs. 10 and 11, respectively. When the proposed technique is not utilized, grid currents contain significant low order harmonic content. These harmonics are generated as the inverter must operate in the over-modulation region to deliver the desired power while also providing negative-sequence compensation. On the other hand, over-modulation is avoided

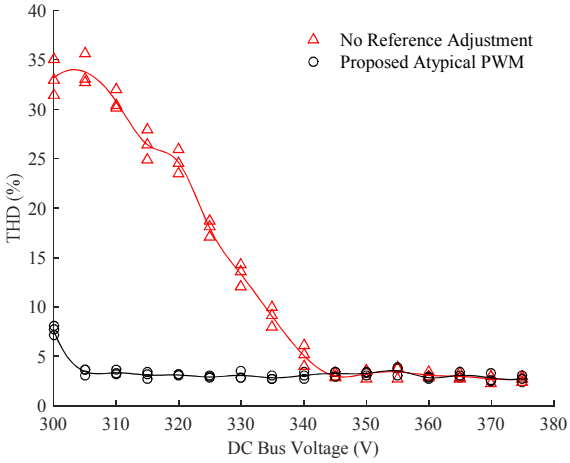


Fig. 12. Plot showing grid current THD vs. $V_{dc}$, with each dc-bus voltage tested at three different measurement times.

for the same dc-bus voltage when using the proposed scheme, demonstrating increased dc-bus utilization.

To further demonstrate increased dc-bus utilization when utilizing the proposed technique, grid currents were measured as the dc-bus voltage of the inverter was decreased in 5 V steps from 375 V to 300 V. Note that the dc-bus voltage was changed to demonstrate the effectiveness of the atypical PWM scheme in maximizing dc-bus utilization, since ratings of the laboratory equipment limited the maximum output power the 2L-VSI could provide. Grid currents drawn, both with and without using the proposed atypical PWM method, were measured at three separate occasions to take into account for grid variations. The average THD of the three measured currents was then computed for both PWM schemes. The results, shown in Fig. 12, demonstrate that utilization of the proposed atypical PWM scheme results in a lower THD for a larger range of dc-bus voltages, demonstrating that the atypical PWM scheme extends the linear modulation range. This increased linear modulation range means that implementation of the proposed method increases the maximum active- and reactive-power that the inverter can provide for a given dc-bus voltage.

## VI. Conclusion and Future Work

An atypical PWM method for microgrid-interactive 2L-VSI operating in unbalanced conditions has been presented in this paper. The proposed technique injects PWM references with a common-mode component computed based on instantaneous reference values. The validity of the proposed switching scheme has been verified through both simulation and experimental studies. It has been shown that the atypical scheme facilitates the injection of active power when the inverter provides negative-sequence compensation as an ancillary service. The proposed technique maximizes dc-bus utilization by maximizing the positive-sequence component PWM references can contain, thereby maximizing the power that the inverters can supply. As future work, the authors expect to analyze the proposed PWM scheme under other ancillary services, such as harmonic compensation.

## References


[1] R. H. Lasseter, "Smart distribution: coupled microgrids," in *Proc. IEEE*, vol. 99, no. 6, pp. 1074-1082, Jun. 2011.

[2] N. Pogaku, M. Prodanovic, and T. C. Green, "Modeling, analysis and testing of autonomous operation of an inverter-based microgrid," *IEEE Trans. Power Electron.*, vol. 22, no. 2, pp. 613-625, March 2007.

[3] J. Rocabert, A. Luna, F. Blaabjerg, and P. Rodríguez, "Control of power converters in ac microgrids," *IEEE Trans. Power Electron*., vol. 27, no. 11, pp. 4734–4749, Nov. 2012.

[4] M. M. Hashempour, M. Savaghebi, J. C. Vasquez, and J. M. Guerrero, "A control architecture to coordinate distributed generators and active power filters coexisting in a microgrid," *IEEE Trans. Smart Grid*, vol. 7, no. 5, pp. 2325–2336, Sep. 2016.

[5] I X. Zhou, F. Tang, P. C. Loh, X. Jin, and W. Cao, "Four-leg converters with improved common current sharing and selective voltage-quality enhancement for islanded microgrids," *IEEE Trans. Power Del*., vol. 31, no. 2, pp. 522–531, Apr. 2016.

[6] M. Hamzeh, H. Karimi, and H. Mokhtari, "Harmonic and negative-sequence current control in an islanded multi-bus MV microgrid," *IEEE Trans. Smart Grid*, vol. 5, no. 1, pp. 167-176, Jan. 2014.

[7] A. E. Leon, J. M. Mauricio, J. A. Solsona, and A. Gomez-Exposito, "Software sensor-based STATCOM control under unbalanced conditions," *IEEE Trans. Power Del.*, vol. 24, no. 3, pp. 1623-1632, Jul. 2009.

[8] S. Du, J. Liu, J. Lin, and Y. He, "A novel DC voltage control method for STATCOM based on hybrid multilevel H-bridge converter," *IEEE Trans. Power Electron.*, vol. 28, no. 1, pp. 101-111, Jan. 2013.

[9] B. Singh, and V. Verma, "Selective compensation of power-quality problems through active power filter by current decomposition," *IEEE Trans. Power Del.*, vol. 23, no. 2, pp. 792-799, Apr. 2008.

[10] P. Acuña, L. Morán, M. Rivera, J. Dixon, and J. Rodriguez, "Improved active power filter performance for renewable power generation systems," *IEEE Trans. Power Electron.*, vol. 29, no. 2, pp. 687-694, Feb. 2014.

[11] F. Nejabatkhah, Y. W. Li, and B. Wu, "Control strategies of three-phase distributed generation inverters for grid unbalanced voltage compensation," *IEEE Trans. Power Electron.*, vol. 31, no. 7, pp. 5228-5241, July 2016.

[12] N. R. Tummuru, M. K. Mishra, and S. Srinivas, "An improved current controller for grid connected voltage source converter in microgrid applications," *IEEE Trans. Sustain. Energy*, vol. 6, no. 2, pp. 595-605, Apr. 2015.

[13] N. M. Dehkordi, N. Sadati, and M. Hamzeh, "A robust backstepping high-order sliding mode control strategy for grid-connected DG units with harmonic/interharmonic current compensation capability," *IEEE Trans. Sustain. Energy*, vol. 8, no. 2, pp. 561-572, Apr. 2017.

[14] R. Chilipi, N. Al Sayari, K. Al Hosani, and A. R. Beig, "Control scheme for grid-tied distributed generation inverter under unbalanced and distorted utility conditions with power quality ancillary services," *IET Renew. Power Gener.*, vol. 10, no. 2, pp. 140-149, Feb. 2016.

[15] A. Hintz, U. R. Prasanna and K. Rajashekara, "Comparative study of the three-phase grid-connected inverter sharing unbalanced three-phase and/or single-phase systems," *IEEE Trans. Ind. Appl.*, vol. 52, no. 6, pp. 5156-5164, Nov.-Dec. 2016.

[16] A. M. Hava and N. O. Çetin, "A generalized scalar PWM approach with easy implementation features for three-phase, three-wire voltage-source inverters," *IEEE Trans. Power Electron.*, vol. 26, no. 5, pp. 1385–1395, May 2011.

[17] J. Chen, Y. He, S. U. Hasan, and J. Liu, "A comprehensive study on equivalent modulation waveforms of the SVM sequence for three-level inverters," *IEEE Trans. Power Electron*., vol. 30, no. 12, pp. 7149–7158, Dec. 2015.

[18] J. S. S. Prasad, R. Ghosh, and G. Narayanan, "Common-mode injection PWM for parallel converters," *IEEE Trans. Ind. Electron.*," vol. 62, no. 2, pp. 789-794, Feb. 2015.

[19] C. N. Bhende, S. Mishra, and S. G. Malla, "Permanent magnet synchronous generator-based standalone wind energy supply system," *IEEE Trans. Sustain. Energy*, vol. 2, no. 4, pp. 361-373, Oct. 2011.

[20] P. S. Moses, and M. A. S. Masoum, "Three-phase asymmetric transformer aging considering voltage-current harmonic interactions, unbalanced nonlinear loading, magnetic couplings, and hysteresis," *IEEE Trans. Energy Convers.*, vol. 27, no. 2, pp. 318-327, June 2012.

[21] F. Blaabjerg, R. Teodorescu, M. Liserre, and A. V. Timbus, "Overview of control and grid synchronization for distributed power generation systems," *IEEE Trans. Ind. Electron.*, vol. 53, no. 5, pp. 1398–1409, Oct. 2006.

[22] A. Timbus, M. Liserre, R. Teodorescu, P. Rodriguez, and F. Blaabjerg, "Evaluation of current controllers for distributed power generation systems," *IEEE Trans. Power Electron.*, vol. 24, no. 3, pp. 654–664, Mar. 2009.

[23] J. Lamb, A. Singh, and B. Mirafzal, "Rapid implementation of solid-state based converters in power engineering laboratories," *IEEE Trans. Power Syst*., vol. 31, no. 4, pp. 2957–2964, Jul. 2016.

[24] J. Lamb, B. Mirafzal, and F. Blaabjerg, "PWM common mode reference generation for maximizing the linear modulation region of CHB converters in islanded microgrids," *IEEE Trans. Ind. Electron*., vol. PP, no. 99, pp. 1-1, Nov. 2017.